Cell Reports

Resource

Gene Expression Architecture of Mouse Dorsal and Tail Skin Reveals Functional Differences in Inflammation and Cancer

Graphical Abstract

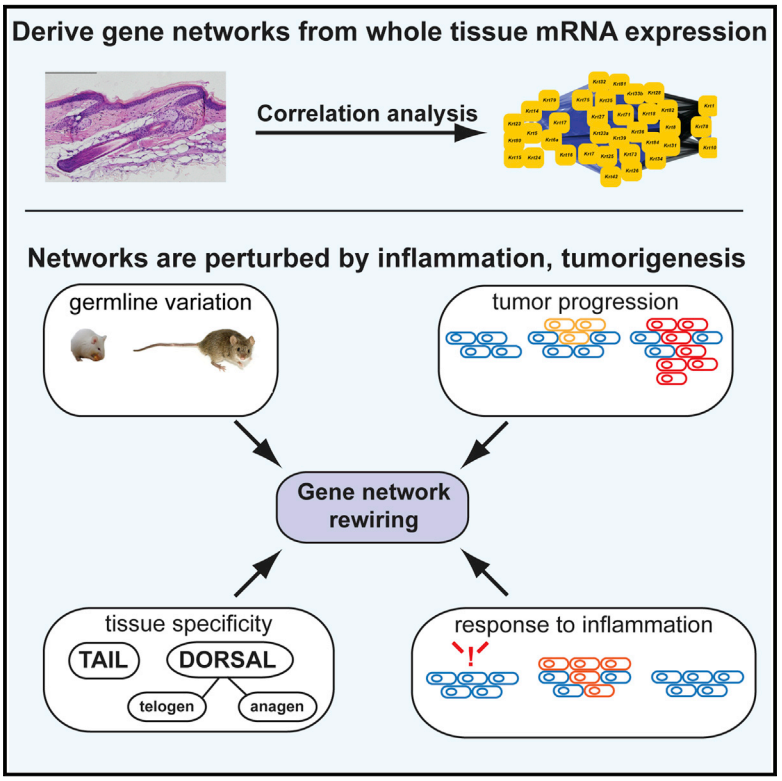

Authors

David A. Quigley, Eve Kandyba, Phillips Huang, ..., Reyno Delrosario, Atul Kumar, Allan Balmain

Correspondence

abalmain@cc.ucsf.edu

In Brief

The demands placed on human skin vary by physical location on the body, producing location specificity in cellular composition, signaling pathways, and response to perturbation, including differential susceptibility to inflammation and disease. Quigley et al. show how skin gene networks respond to perturbation by genetic variation, inflammation, and tumorigenesis.

Highlights

- Gene expression networks reconstruct the cellular composition of a complex tissue
- Genetic influence on gene expression varies by tissue location in the skin
- Smoothened pathway activity is rewired between tail and dorsal skin
- Gene expression networks are rewired in premalignant tumors and again in carcinoma

Accession Numbers

GSE52650

Quigley et al., 2016, Cell Reports *16*, 1153–1165
July 26, 2016
http://dx.doi.org/10.1016/j.celrep.2016.06.061

CellPress

Cell Reports
Resource

Gene Expression Architecture of Mouse Dorsal and Tail Skin Reveals Functional Differences in Inflammation and Cancer

David A. Quigley,[1,2,3,4] Eve Kandyba,[1] Phillips Huang,[1,5] Kyle D. Halliwill,[1] Jonas Sjölund,[1,6] Facundo Pelorosso,[1,7] Christine E. Wong,[8] Gillian L. Hirst,[1] Di Wu,[1] Reyno Delrosario,[1] Atul Kumar,[1] and Allan Balmain[1,9,*]
[1]Helen Diller Family Comprehensive Cancer Center, University of California, San Francisco, San Francisco, CA 94158, USA
[2]Department of Genetics, Institute for Cancer Research, Oslo University Hospital, The Norwegian Radium Hospital, Oslo 0310, Norway
[3]K.G. Jebsen Centre for Breast Cancer Research, Institute for Clinical Medicine, Faculty of Medicine, University of Oslo, Oslo 0313, Norway
[4]Department of Epidemiology and Biostatistics, University of California, San Francisco, San Francisco, CA 94158, USA
[5]Genome Institute of Singapore, 60 Biopolis Street, #02-01 Genome Building, Singapore 138672, Singapore
[6]Division of Translational Cancer Research, Department of Laboratory Medicine, Lund University, 22381 Lund, Sweden
[7]Instituto de Farmacología, Facultad de Medicina, Universidad de Buenos Aires, Paraguay 2155, 9th Floor, Ciudad Autónoma de Buenos Aires 1121, Argentina
[8]Institute of Surgical Pathology, University Hospital Zurich, 8091 Zurich, Switzerland
[9]Department of Biochemistry and Biophysics, University of California, San Francisco, San Francisco, CA 94158, USA
*Correspondence: abalmain@cc.ucsf.edu
http://dx.doi.org/10.1016/j.celrep.2016.06.061

SUMMARY

Inherited germline polymorphisms can cause gene expression levels in normal tissues to differ substantially between individuals. We present an analysis of the genetic architecture of normal adult skin from 470 genetically unique mice, demonstrating the effect of germline variants, skin tissue location, and perturbation by exogenous inflammation or tumorigenesis on gene signaling pathways. Gene networks related to specific cell types and signaling pathways, including sonic hedgehog (*Shh*), *Wnt*, *Lgr* family stem cell markers, and keratins, differed at these tissue sites, suggesting mechanisms for the differential susceptibility of dorsal and tail skin to development of skin diseases and tumorigenesis. The *Pten* tumor suppressor gene network is rewired in premalignant tumors compared to normal tissue, but this response to perturbation is lost during malignant progression. We present a software package for expression quantitative trait loci (eQTL) network analysis and demonstrate how network analysis of whole tissues provides insights into interactions between cell compartments and signaling molecules.

INTRODUCTION

The skin is the largest human organ, forming an essential barrier against environmental insults, including physical and chemical exposures. Skin is the tissue of origin of the commonest form of cancer in white populations (Diepgen and Mahler, 2002) as well as a host of other diseases ranging from relatively common inflammatory conditions, such as atopic dermatitis, to rare life-threatening conditions, such as the skin fragility syndrome epidermolysis bullosa. Studies both in mice and in humans have uncovered the underlying genetic basis of many skin diseases and have led to pioneering discoveries in tissue transplantation, regeneration, and stem cell biology (Blanpain and Fuchs, 2006). Keratinocytes, the most common cell type in skin, produce several closely related families of proteins with distinctive locations and functions (Fuchs, 1995; Schneider et al., 2009). Keratins were initially characterized as structural proteins that form the cytoskeletal architecture (Steinert et al., 1985), but they can also function in signaling pathways in skin in response to tissue perturbation (Arwert et al., 2012; Gu and Coulombe, 2007; Paramio and Jorcano, 2002).

Skin morphology, function, and tumor susceptibility vary in different parts of the body (Rinn et al., 2008). To withstand physical stress, the soles of human feet, mouse paws, and mouse tails have thicker and tougher epidermal layers than dorsal skin. Mouse dorsal skin, but not tail skin, is highly sensitized to squamous papilloma development induced by chemical initiators and promoters of carcinogenesis (Schweizer and Marks, 1977b). Exposing *Ptch1*$^{+/-}$ mice to ionizing radiation produces basal cell carcinomas (BCCs) in dorsal skin (Wang et al., 2011). In contrast, activation of the hedgehog pathway by oncogenic smoothened (*Smo*) driven by widely expressed *Krt14*-Cre results in development of BCCs preferentially in mouse tail skin (Youssef et al., 2012). Similarly, overexpression of *Gli2* using a *Krt5* promoter also led to development of BCCs in the tail skin (Grachtchouk et al., 2000). The underlying basis of these site-specific phenotypes is not presently understood.

In this study, we identify significant differences in the network architecture of signaling pathways between mouse dorsal and tail skin using gene expression quantitative trait loci (eQTL) and differential correlation analysis. We performed this analysis in a cohort of 470 genetically distinct animals produced by crossing FVB/N and *Mus spretus* mice, two highly divergent strains. We analyzed differential gene expression networks after stimulation of inflammation and epithelial proliferation using the tumor

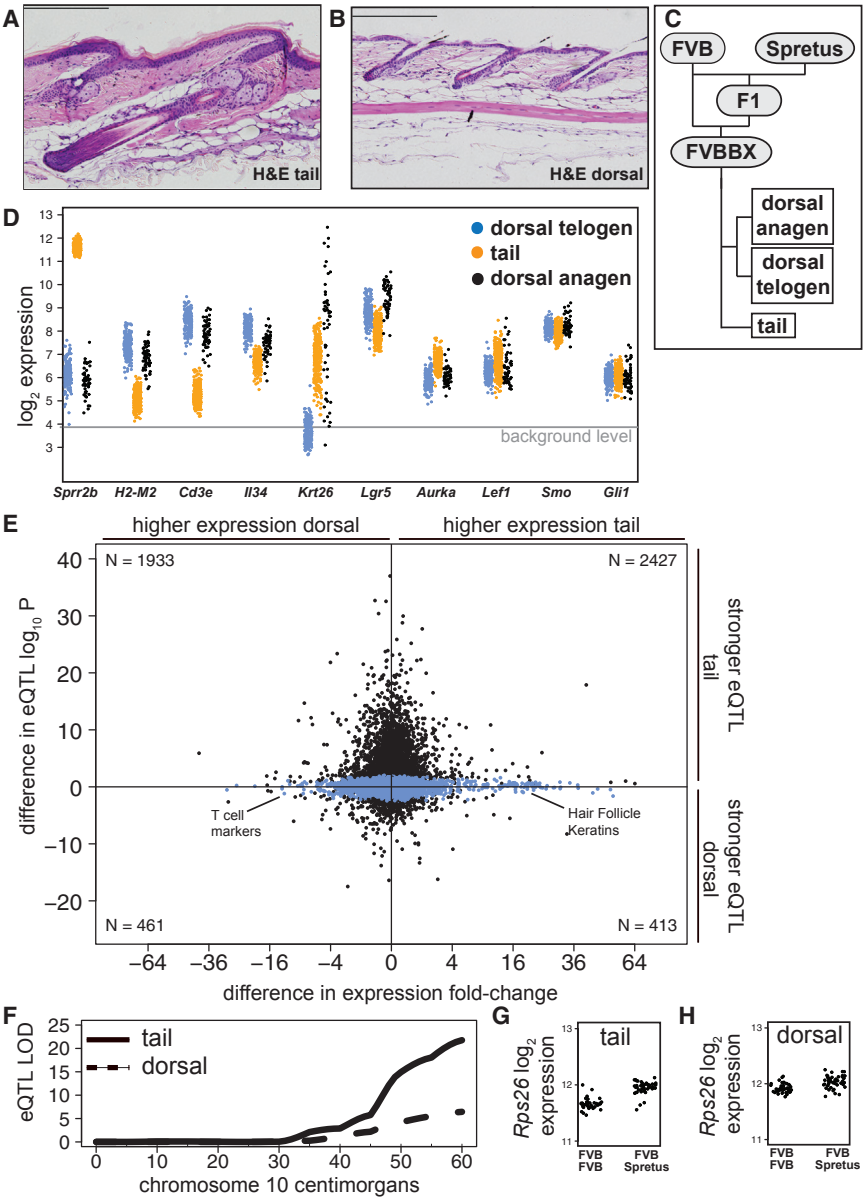

Figure 1. Synchronized Expression of Major Signaling Pathways in Dorsal Skin

(A and B) H&E stain of (A) tail skin and (B) dorsal skin from an 8-week-old mouse. Scale bars indicate 500 μM.

(C) Outline of the FVBBS breeding scheme and tissues obtained.

(D) Gene expression levels of key genes in tail, dorsal anagen, and dorsal telogen skin.

(E) Scatterplot comparing the difference in eQTL effect size for each probeset in tail and dorsal samples (y axis) with the difference in mean expression levels in tail and dorsal samples (x axis). Probes with significant eQTL in either tail or dorsal skin drawn are in black but otherwise drawn in blue. The genes with the largest increase in eQTL strength tended to have the smallest change in gene expression levels.

(F) Statistical strength of the eQTL for *Rps26* in tail skin (solid line) and dorsal skin (dashed line) on chromosome 10.

(G and H) Expression of *Rps26* in tail skin (G) and dorsal skin (H) separated by genotype at chromosome 10 (118 Mb). F/F, homozygous FVB/N; F/S, heterozygous FVB/N/Spret/Ei.

promoter TPA (tetradecanoyl-phorbol acetate) or in tumors induced by sequential treatment with dimethylbenzanthracene (DMBA) and TPA. We also present *CARMEN*, a user-friendly software package for network analysis. We demonstrate how this systems genetics strategy identifies the genes and pathways that are engaged in response to different forms of perturbation. These resources provide opportunities for generation and testing of many specific hypotheses related to skin biology.

RESULTS

Gene Expression Networks Reconstruct the Cellular Composition of the Skin

Adult mouse dorsal skin in the resting (telogen) phase has thin cornified and epithelial layers and small, densely packed hair follicles, while mouse tail skin has a thick and scaled cornified envelope layer and large, sparsely placed anagen hair follicles (Schweizer and Marks, 1977a) (Figures 1A and 1B). To investigate the genetic basis of the skin site-specific biological differences, we measured gene expression in 222 dorsal skins and 248 tail skins from a backcross of 8-week-old *Mus musculus* (FVB/N) and *Mus spretus* mice, referred to as FVBBX mice (Figure 1C; Experimental Procedures). Tail skins had significantly higher expression of genes expressed in the outer cornified layer of the skin such as small proline receptor 2b (*Sprr2b*; Figure 1D). Individual hair follicles cycle through periods of growth (anagen) and destruction (catagen), with an intervening period of quiescence (telogen) (Stenn and Paus, 2001). Hair follicle cycling affects the skin's physical structure and its susceptibility to experimental models of carcinogenesis (Mancuso et al., 2006; Miller et al., 1993). In the first 2 months after a mouse is born, its dorsal hair follicles progress synchronously through this cycle in a temporally predictable manner (Müller-Röver et al., 2001). Expression of hair-follicle inner-root-sheath-specific keratins such as *Krt26* was at or below background levels in 77% of the dorsal skin samples (Figure 1D), indicating that follicles in these skins were in telogen. All tail samples expressed hair-follicle-specific keratins at levels above background, consistent with follicles in tail being primarily in the anagen phase (Figures 1A and 1D).

Expression of mitotic markers such as Aurora kinase A (*Aurka*) was significantly higher in tail than in dorsal telogen or anagen

skin (Figure 1D), consistent with elevated proliferation rates. In agreement with prior observations of site-specific immune responses in the skin (Bergstresser et al., 1980; Nabors and Farrell, 1994; Tong et al., 2014), tail skin showed dramatically reduced expression of markers of tissue-resident Langerhans cells such as *Il34* (Wang et al., 2012), genes of the Major Histocompatibility Complex (MHC) such as *H2-m2,* and T cell surface markers such as *Cd3e* (Figure 1D). The highest expression of these genes in dorsal was during telogen phase (Figure 1D), confirming measurements made by Paus and colleagues (Paus et al., 1998).

The Genetic Influence on Energy and Metabolism Gene Expression Is Stronger in Tail Skin

We hypothesized that the genetic architectures of tail and dorsal skin would differ in ways that reflect their distinct forms and functions. To test this idea, we performed an eQTL study in the 89 FVBBX mice where we had both dorsal skin and tail skin from the same animal. Gene expression data were corrected for strain-specific SNP effects on microarray hybridization (Experimental Procedures). Using matched tissues reduced non-genetic variation and provided equivalent statistical power in both conditions. Surprisingly, we identified 4,753 genes with significant eQTL in tail skin but only 1,710 genes with significant eQTL in dorsal skin.

One possible explanation for this result would be if cell populations present preferentially in tail skin were the source of additional significant eQTL in tails. However, the number of genes expressed above background levels was similar in tail and dorsal skin, and only a small number of genes had nearly complete tissue-specific expression. Although most genes were significantly differentially expressed between matched tail and dorsal skin, the effect size was usually very small (median fold change 6% higher in tail; Figure 1E). Genes with large location-specific differences in expression did not tend to have large differences in eQTL strength. Intermediate filament keratins in the hair follicle network such as *Krt26* had the highest relative mean expression levels in tail skin (Figure 1E), reflecting the fact that most matched dorsal skin samples were in telogen. Many of the genes with highest relative expression in dorsal skin were T cell surface markers such as *Cd3e* (Figure 1D). However, the eQTL strength of these hair follicle keratins and T cell markers was similar in both tail and dorsal skin (Figure 1E). There was not a significant correlation between the difference in gene expression levels and the difference in eQTL strength. The peaks of almost all eQTL mapped to the same locus in tail and dorsal skin samples, and after increasing the number of samples in the tail eQTL analysis from 89 to 248 by adding additional unmatched FVBBX animals, we did not identify more than a handful of genes with eQTL exclusively in dorsal skin. These results suggest the tissue locations differed in linkage strength but not in their genetic architecture.

Gene Ontology enrichment analysis indicated that genes with the largest increase in eQTL strength ($-\log_{10}$P increase $\geq$ 10) were significantly enriched for roles in the mitochondria, cellular metabolism, translation, and energy production. These genes usually had very small differences in expression levels. One example was *Rps26,* a ribosomal protein mutated in Diamond-Blackfan anemia, which can affect TP53 transactivation (Cui et al., 2014; Doherty et al., 2010). *Rps26* was expressed at nearly identical levels in tail and dorsal skin but was under much stronger genetic control in tail skin (logarithm of the odds $[LOD]_{tail}$ 21.8 versus LOD_{dorsal} 6.4; Figures 1F–1H). We interpret this to mean that the increase in tail eQTL strength was not simply the result of cell populations present in the tail skin and absent in dorsal skin, or the result of higher expression levels producing stronger linkage signals. Rather, these differences reflect differences in the activity of genes linked to protein production and cellular metabolism. This was concordant with the observation that levels of mitotic genes such as Aurora kinase A are expressed at constitutively higher levels in tail skin (Figure 1D).

Conserved and Tissue-Specific Networks in Dorsal and Tail Skins

Signals from the Wnt and hedgehog pathways organize the hair placode during mouse embryonic development, and Wnt activation from the dermal papillae is required for follicle down-growth and cycling (Chiang et al., 1999; Gat et al., 1998; Huelsken et al., 2001; Kishimoto et al., 2000; St-Jacques et al., 1998). Expression of the Wnt-associated transcription factor *Lef1* (DasGupta and Fuchs, 1999) was modestly higher in tail skin and dorsal anagen skin than in dorsal telogen, but expression levels of the hedgehog pathway genes *Smo* and *Gli1* were nearly identical between these tissues (Figure 1D). Gene expression correlation analysis can reveal features of signaling networks that are not detectable by measuring differential expression levels between tissues. Correlation was among the first statistical tools to be applied to microarray data to identify sets of genes that act in concert (Chu et al., 1998). In contrast, relatively few studies have exploited how the differences in correlation between contrasting conditions can elucidate the changes in how genes work together under different biological conditions. Several groups have developed formal methods to analyze differential correlation (reviewed in de la Fuente, 2010). Some methods determine whether pre-specified gene sets are differently correlated in two conditions (Braun et al., 2008; Choi and Kendziorski, 2009), while others discover gene sets directly from the data (Watson, 2006). We used CARMEN to calculate differential correlation between tail and dorsal telogen tissues (Experimental Procedures). We then calculated pairwise differential correlation genome-wide and ranked each gene by the number of significant differential correlations between the two tissue conditions. The 100 genes with the largest number of rewired correlations was enriched for genes with key roles in Wnt signaling such as *Lef1*, *Fzd1*, *Tnik*, *Rspo3*, and *Lgr5*, as well as genes with key roles in hair follicle stem cell biology such as *Lgr5*, *Msx2*, *Lhx2*, *Hoxb13,* and *Dlx3* (Table S1). The second-most-frequently rewired gene, TRAF2 and NCK interacting kinase (*Tnik*), activates Wnt target genes in intestinal crypts (Mahmoudi et al., 2009) and has a role in Wnt-driven colorectal tumorigenesis (Shitashige et al., 2010). In tail skin, but not dorsal telogen skin, expression of *Tnik* was significantly correlated with expression of *Lef1* and *Gli1* (Figure 2A), whereas in dorsal, but not tail, skin *Tnik* expression was correlated with expression of adherens junctions genes such as e-cadherin (*Cdh1*) and T cell lymphoma invasion and metastasis 1 (*Tiam1*) (Figure 2B). Plotting these gene networks (Figures 2C and 2D) allows the identification of gene pathway

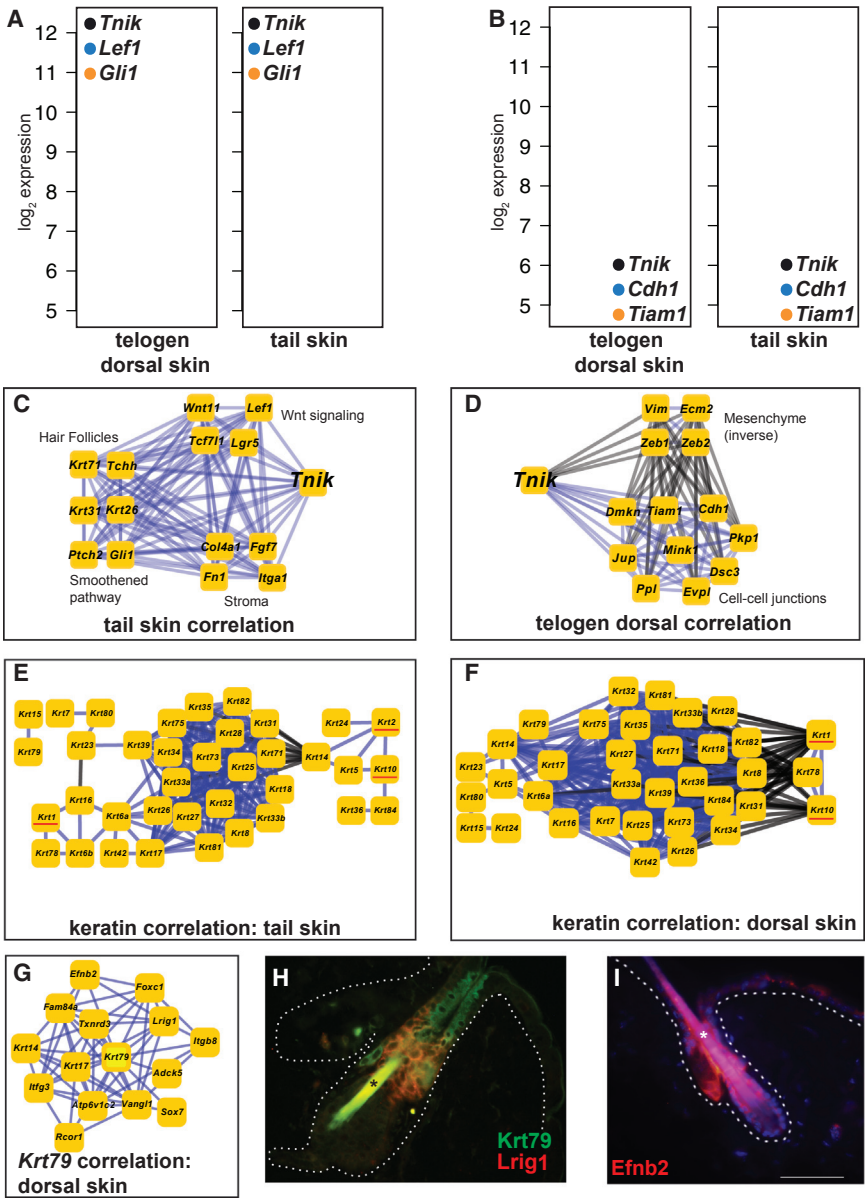

Figure 2. Keratin Correlation Networks in Tail and Dorsal Skin

(A and B) Gene expression levels of (A) *Tnik*, *Lef1*, and *Gli1* and (B) *Tnik*, *Cdh1*, and *Tiam1* in mouse dorsal telogen and tail skin, sorted by increasing *Tnik* expression.

(C and D) Gene expression correlation of genes differentially expressed with *Tnik* expression in tail skin (C) and telogen dorsal skin (D).

(E and F) Gene expression correlation networks for all keratins in tail skin (E) and dorsal skin (F); *Krt1*, *Krt2*, and *Krt10* are underlined where present. Edges connect genes (boxes) with significantly expressed genes; black edges are inverse correlation, and blue edges are direct correlation.

(G) Gene expression correlation network for *Krt79*.

(H and I) Immunofluorescence image for antibodies against (H) Lrig1 (red) and Krt79 (green) in FVB mice and (I) Efnb2.

rewiring that would not be detectable from analysis of gene expression levels alone.

Keratin Gene Expression Networks in Dorsal and Tail Skin

Many skin disorders are caused by germline alterations in genes encoding keratins, resulting in hyperproliferation, epidermal barrier defects, or defective control of epidermal permeability (Lane and McLean, 2004). We hypothesized that network expression analysis could identify rewired gene expression pathways associated with differing susceptibility to disease models. Mutations in *Krt1* and *Krt10* are linked to epidermolytic hyperkeratosis and ichthyosis, rare conditions thT result in blistering and thickening of skin (Cheng et al., 1992; Rothnagel et al., 1992). The palmoplantar variety of hyperkeratosis particularly affects the palms and soles of the feet. The *Dsk2* mutation at *Krt2,* a model for epidermolysis bullosa, results in hyperkeratosis in mouse footpads, ears, and tails, but not dorsal skin (Fitch et al., 2003; Rentrop et al., 1987). Correlation analysis of keratin gene expression in dorsal and tail skin (Figures 2E and 2F; *Krt1*, *Krt2*, and *Krt10* underlined) provided a rationale for the functional significance of tail-specific expression of *Krt2* (Rentrop et al., 1987). Expression of type II keratin *Krt1* and type I keratin *Krt10,* while strongly correlated in dorsal skin, showed no mRNA relationship in tail skin. Although both *Krt10* and *Krt1* were highly expressed at the mRNA level in tails, *Krt10* was significantly correlated only with *Krt2*. In agreement with these data, germline deletion of *Krt2* in the mouse causes acanthosis, hyperkeratosis, and inflammation of the ear and tail, with accumulation of aggregates of Krt10 (Fischer et al., 2014). Correlation network analysis would correctly have predicted that in thickened skin locations such as the tail, *Krt2* substitutes for roles normally played by *Krt1* in barrier function and inflammation.

We further analyzed the mRNA expression network for a keratin that is localized within a specific compartment of the skin. We calculated a correlation network for expression of the type II keratin *Krt79* (Figure 2G), which is expressed in cells that line the infundibulum and co-localizes in part with expression of *Krt17* (Veniaminova et al., 2013). The expression network for *Krt79* included, in addition to *Krt17*, the stem cell marker leucine-rich repeats and immunoglobulin-like domains 1 (*Lrig1*). Importantly, *Lrig1* is a transmembrane protein and a marker of a stem cell that maintains the infundibulum and sebaceous gland, but not the hair follicle or the interfollicular epidermis (Page et al., 2013;

Veniaminova et al., 2013). Immunohistochemical analysis confirmed that Krt79 and Lrig1 protein are both localized within the infundibulum region, but primarily in adjacent cells rather than in exactly the same cell population (Figure 2H).

Expression of *Efnb2* was also significantly correlated with expression of *Krt79* in this network. Since very little is known about possible functions and localization of *Efnb2* in skin, we carried out an immunohistochemical analysis of Efnb2 expression and found that it is also expressed in the infundibulum and sebaceous gland, in a pattern that overlaps with but is more extensive than Krt79 and Lrig1 (Figure 2I). We conclude that analysis of expression networks derived from this heterogeneous mouse population can provide novel information on the localization and possible functional relationships between genes expressed in complex whole tissues in vivo. It is, however, important to note that many of the statistically significant genes within the *Krt79* network may be expressed outside the infundibulum. While it is possible that significantly correlated genes are expressed in the same cells within a tissue compartment or interact within the same signaling pathway, it is also possible that RNA correlations reflect paracrine relationships between adjacent cell types or a hierarchical relationship within a cell lineage.

Network Changes in Response to Inflammatory Agents

It is also possible to visualize network correlations using samples from inbred mice subjected to a strong perturbation such as induction of inflammation. To model epithelial response to inflammation, we treated dorsal skin of inbred FVB mice with the phorbol ester TPA, which results in edema and an influx of inflammatory cells into the skin (Fürstenberger and Marks, 1983; Schlingemann et al., 2003). TPA treatment has been observed to induce differentiation of basal keratinocytes (Reiners and Slaga, 1983). On induction of a wound stimulus, cells positive for the Wnt-responsive stem cell markers Lgr5 and Lgr6 can give rise to progeny that migrate into the epidermis and may contribute to the wound-healing process (Kasper et al., 2011). Correlation network analysis of gene expression across a 1-week time course after a single treatment with TPA (Figure 3A) revealed the coordinated response of cytokines, keratins, and stem cell markers over time. Code to reproduce the analysis and figures in this manuscript is publicly available at http://davidquigley.com/publications.html.

Expression of the immediate response interleukins *Il1b* and *Il6* increased 8- to 16-fold 2 hr after TPA treatment (Figure 3B). The "acute inflammatory response" motif in Figure 3A includes *Il1b* as well as other known early response genes such as *Tgfa*, *Junb*, and *Nfkb2*. Expression of macrophage surface markers such as macrophage scavenger receptor 1 (*Msr1*) peaked at a 5-fold increase after 12 hr, consistent with the influx of macrophages into the treated skin. Within the "Mitosis" network, expression of markers of the M phase of the cell cycle such as *Mki67* decreased immediately after treatment only to rebound to higher-than-baseline levels by 24 hr, in agreement with earlier observations of early decrease in DNA synthesis after TPA treatment, followed by entry into S phase after 12–18 hr (Balmain et al., 1977). Expression of the proliferation-associated keratins *Krt6a*, *Krt6b*, *Krt16*, and *Krt17* increased significantly after TPA treatment, and these genes were linked to the "Skin Barrier and Cornified Envelope" module. Expression of the Wnt signaling agonist *Rspo3* and Wnt effector *Lef1* was significantly decreased by TPA treatment, with *Rspo3* expression gradually recovering after acute inflammatory stimulus (Glinka et al., 2011).

We summarize the kinetics of epithelial response to TPA exposure using markers of stem, basal, suprabasal, and terminally differentiated cells in Figure 3C. Bulge stem cell markers (*Lgr5*) drop immediately by 4-fold and slowly recover to baseline levels by 72 hr. Early differentiation markers (involucrin) increased to a peak at 2 hr, followed by markers of the primitive epithelium (*Krt8*), which increase to peak at 6 hr and revert to homeostatic levels by 12 hr. The suprabasal epithelium (*Krt1*) shows the inverse trend, decreasing at 6 hr and recovering by 24 hr. Markers of the cornified envelope (*Sprr1b*) and keratin wound response (*Krt6a*) increase to a peak at 12 hr and are still significantly elevated 48 hr after treatment. These observations are compatible with an immediate differentiation response to TPA by primitive cells and suprabasal cells, followed by an increase in basal cell production to replenish the suprabasal cell population between 12 and 24 hr after treatment. The early drop in mitotic gene expression suggested the increase in involucrin and *Sprr1b* expression was the result of a direct induction of a differentiation response rather than a consequence of proliferation. Our observations are compatible with earlier morphological and biochemical observations of the effects of TPA on mouse skin, which showed an early induction of differentiation markers and a change in the balance of basal and suprabasal cells following TPA treatment (Reiners and Slaga, 1983).

Keratin Gene Networks Linked to Pachyonychia Congenita

Germline mutations in *Krt6a*, *Krt6b*, *Krt16*, and *Krt17* are all linked to the rare skin disease pachyonychia congenita (PC), a congenital disorder characterized by blisters, thickened nails, and hyperkeratosis (Bowden et al., 1995; McLean et al., 1995). Network analysis revealed strong correlations between these mRNA levels of these genes under normal and inflammatory conditions, suggesting coordinated functions in skin architecture. The type II keratins Krt6a and Krt6b are thought to heterodimerize with the type I keratin Krt16, but in normal dorsal skin, expression of *Krt16* was significantly correlated with expression of *Krt6a*, but not *Krt6b* (Figure 2F), suggesting preferential heterodimerization between *Krt16* and *Krt6a* compared to *Krt6b*, while in normal tail skin, expression of *Krt16* was linked to expression of both *Krt6a* and *Krt6b* (Figure 2E). To our knowledge, there are currently no antibodies that can reliably distinguish Krt6a from Krt6b to address the question of differential binding under these conditions. After TPA treatment, the *Krt16* expression profile was significantly correlated with that of *Krt6b*, as well as *Krt6a* and barrier/inflammation genes such as *S100a8*, *Lce3a*, and small proline receptors *Sprr2e* and *Sprr2d* (Table S2). There was also significant differential correlation between expression of *Krt16* and *S100a8*, *Defb3*, and other genes induced by TPA exposure when comparing untreated FVBBX tail skin to dorsal skin (Table S3). The tail-specific correlation of *Krt16* with other genes induced during wound response, as well as elevated constitutive expression of *Krt16* in normal tail,

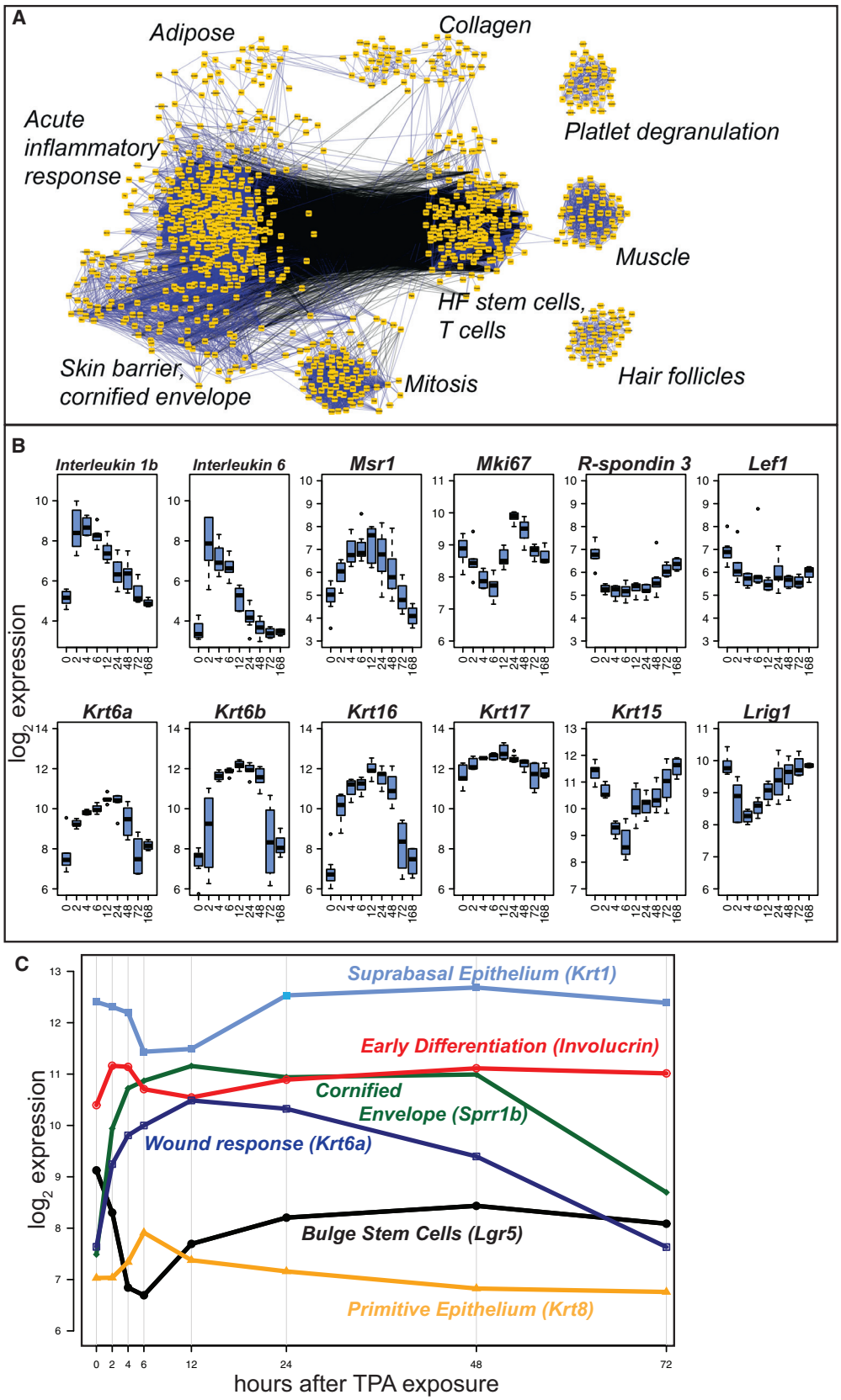

(legend on next page)

was compatible with elevated keratinocyte proliferation in tail skin and was reminiscent of the wound response seen in TPA-treated dorsal skin. These observations are consistent with previous analysis of data from the tail skins of aged (>1 year old) tumor-bearing mice, which implicated *Krt16* in regulation of innate immune responses to barrier dysfunction (Lessard et al., 2013).

Network analysis of *Krt17* in normal tail skin, in contrast to the analysis of *Krt16*, showed no significant correlations with *S100a8* or other markers of acute inflammatory responses but was linked to expression of hair follicle keratins (Tables S4 and S5; Figures 2E and 2F). In dorsal skin, *Krt17* was correlated with a number of epidermal stem cell markers (e.g., *Sox9*, *Dlx3*, and *Tbx1*) as well as *Krt6a* but only weakly with *Krt16*. However, all of the genes that play causative roles in PC (*Krt6*a, *Krt6b*, *Krt16*, and *Krt17)* were significantly correlated with each other after treatment of skin with TPA, indicating that these genes form part of a coordinated network response to inflammation and tissue regeneration.

Smoothened Activity Is Rewired between Tail and Dorsal Skin

Skin tumorigenesis studies have shown differences in susceptibility of tail and dorsal skin to induction of BCCs by activation of the Shh signaling pathway. We hypothesized that tissue-specific regulation of Smoothened is responsible for the observation that models of BCC that activate Smoothened only produce tumors on the tail skin. It has previously been reported that Smo protein is absent in tail follicles (Wang et al., 2011). We first performed immunostaining for Smo protein with the antibody used by Wang and colleagues (Wang et al., 2011). In agreement with their results, we detected cytoplasmic Smo protein at the inner root sheath of dorsal anagen follicles (Figures 4A and 4B). In contrast to the previous report, we also detected Smo protein at the base of tail follicles (Figures 4C and 4D). Specificity of Smo staining was confirmed by staining Smo induced by the $Ptch^{+/-}$ radiation model (Figure S1). We then co-stained for Smo protein and EGFP in mice expressing EGFP at the endogenous Lgr5 locus. Dorsal telogen skin showed Lgr5-positive cells at the dermal papilla, but no Smo protein, as expected (Figure 4E). Tail skin showed co-localization of Lgr5 and Smo protein in cells between the dermal papilla and bulge region (Figure 4F), thus confirming that Smo is in fact expressed in tail skin during anagen.

Our data show that Smo protein is expressed in both dorsal and tail skin and furthermore that the average level of Smoothened mRNA expression is nearly identical in skin from both sites (Figure 1D). However, we found 676 genes with significant differential correlation with Smoothened in these tissues ($p < 0.05$, Bonferroni correction, see Experimental Procedures). Gene Ontology enrichment analysis indicated significant activation of correlation in tails between expression of Smoothened and both canonical Wnt receptor signaling ($p < 6 \times 10^{-5}$) and the hair follicle cycle ($p < 2 \times 10^{-5}$). We plotted correlation between key genes in these networks, illustrating that while there was a constitutive association between expression levels of *Lef1* and hedgehog genes *Gli1* and *Ptch1* in both compartments, the association between *Smo* and the Wnt and hair follicle gene networks was restricted to tail skin (Figures 4G and 4H). We conclude that constitutive expression of a tail network encompassing *Smo* and components of the *Wnt-Lef1* signaling pathway may explain the development of BCCs preferentially in the tail in spite of widespread targeting of mutant Smo to multiple body sites, including dorsal skin, using the *Krt14* promoter (Wong and Reiter, 2011; Youssef et al., 2010).

Rewiring of Tumor Suppressor Gene Networks during Premalignancy

We then applied differential correlation analysis to identify how relationships between genes are altered during tumorigenesis, analyzing previously published gene expression measurements on normal skin, benign tumors, and malignant tumors (Quigley et al., 2009; Quigley et al., 2011). Skin tumors were induced on mice using a two-stage skin carcinogenesis protocol as previously described; briefly, tumors were initiated using DMBA, which induces oncogenic mutations in *Hras1* (Quintanilla et al., 1986), and were then promoted with TPA, resulting in benign papillomas, some of which progress to malignant invasive carcinomas.

The most frequently differentially correlated genes when comparing normal skin to benign tumors were the ribosomal protein *Rps7* and phosphatase and tensin homolog deleted on chromosome 10 (*Pten*). Both genes were robustly expressed in skin, papillomas, and carcinomas, with mean change in expression levels between matched normal skin and papillomas of <20%. Analysis based on differential expression would not suggest that these genes are of special interest during tumorigenesis. However, these genes are both linked to tumor suppressor pathways potentially activated in epithelial tumors. *Rps7* binds directly to Mdm2, inhibiting its ability to degrade p53 (Zhu et al., 2009). *Pten* is an antagonist of the PI3-kinase signaling pathway, which is frequently inactivated in epithelial tumors (Salmena et al., 2008). Mice with heterozygous knockouts of *Pten* develop spontaneous tumors; mice with heterozygous or homozygous knockout of *Pten* targeted to their keratinocytes show a dose-dependent increase in spontaneous skin tumor formation and susceptibility to DMBA/TPA treatment (Suzuki et al., 2003). We have previously shown that 70% of the carcinomas that arise in $Pten^{+/-}$ mice after DMBA/TPA treatment do not have an *Hras* mutation, but all of these tumors lost their wild-type *Pten* allele. Wild-type animals treated with DMBA/TPA did not lose *Pten* copies or develop somatic *Pten* mutations in papilloma genomic DNA (Mao et al., 2004). These previous data identified a specific, mutually exclusive relationship between *Hras* mutations and

Figure 3. Keratin Correlation and TPA Response Networks

(A) Gene expression correlation network for genes with significantly correlated response in dorsal skin to TPA exposure.

(B) Box plots of gene expression in dorsal skin at baseline (0 hr) and at time points from 2 hr to 1 week after TPA treatment. Number of animals for each time point was 9 (0 hr), 6 (2 hr), 4 (4 hr), 7 (6 hr), 6 (12 hr), 7 (24 hr), 8 (48 hr), 4 (72 hr), and 4 (1 week).

(C) Mean expression levels of *Krt1*, *Involucrin*, *Sprr1b*, *Krt6a*, *Lgr5*, and *Krt8* in the TPA treatment experiment, with the x axis plotted to scale for number of hours since treatment.

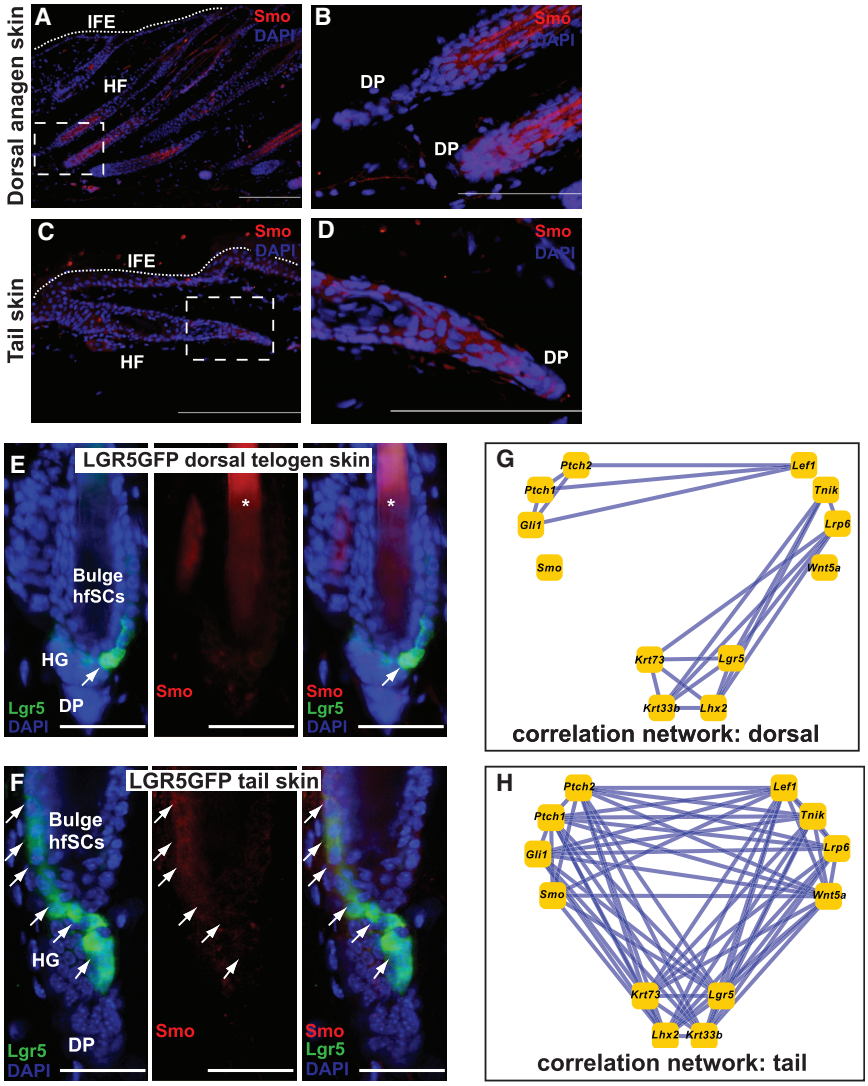

Figure 4. Rewired Hedgehog Networks in Tail and Dorsal Hair Follicles

Correlation networks for key hedgehog, Wnt, and hair follicle genes in (C) dorsal and (D) tail skin. Lines connect significantly correlated gene pairs.

(A–D) Mouse skin immunostained with an anti-SMO antibody (red) and counter-stained with DAPI (blue). SMO protein was present in (A) dorsal anagen follicles (B shows higher magnification of the dashed box) and (C) tail follicles (D, higher magnification) most prominently near the dermal papillae. Lower- and higher-magnification scale bars indicate 500 and 200 μM, respectively.

(E and F) LGR5-EGFP dorsal telogen mouse skin (E) and tail skin (F) immunostained with an anti-SMO antibody (red) and anti-EGFP antibody (green) and counterstained with DAPI (blue). Scale bar is 50 μM, and images were taken at 40×.

(G and H) Correlation networks for key hedgehog, Wnt, and hair follicle genes in dorsal skin (G) and tail skin (H), illustrating the tail-skin-specific correlation between expression of *Smo* and expression of the Wnt and hair follicle networks. Lines connect significantly correlated gene pairs.

Pten signaling in mouse skin. This relationship is supported by the observation that across the whole genome, *Pten* was the third most frequently "rewired" genes in papillomas carrying *Hras* mutations. Several of the genes that acquire correlations with *Pten* in papillomas are involved in alternative tumor suppressor pathways (Table S6), suggesting that this rewiring is part of a concerted response to perturbation induced by activation of *Ras* signaling.

In many cases, the significant correlations with *Pten* that were acquired in premalignant papillomas were subsequently lost during malignant progression to carcinomas. This was the case with *Pten* and the transforming growth factor beta (TGF-β) signaling mediator SMAD family member 4 (*Smad4*), which is a well-characterized tumor suppressor gene both in mouse and human tumors (Figures 5A–5C). Keratinocyte-specific inactivation of *Smad4* blocks hair follicle differentiation and cycling and leads to invasive squamous cell carcinomas, while deletion of both *Smad4* and *Pten* results in accelerated tumorigenesis (Yang et al., 2005). Moreover, *Smad4* and *Pten* synergize to prevent pancreatic ductal adenocarcinoma (Ding et al., 2011; Xu et al., 2010).

Pten and Smad4 proteins are expressed in the epithelial layer of normal dorsal skin with diffuse cytoplasmic staining (Figures 5D and 5F). In contrast, in papillomas, Pten protein is expressed at moderately elevated levels in the membranes of epithelial cells, a location compatible with its known activity on the cell membrane (Figure 5E), while Smad4 protein is expressed at moderately higher levels in the nucleus. Our results suggest that even in the absence of inactivating mutations in *Pten* (McCreery et al., 2015), genetic networks are rewired to activate tumor suppressor pathways in benign tumors as a response to activated Ras signaling. Carcinomas, however, no longer show this activated response pattern, suggesting that alternative genetic or epigenetic mechanisms lead to loss of these growth controlling pathways during tumor progression.

DISCUSSION

Human skin is a self-renewing tissue that has evolved specific functions according to location in the body. These functions may require the presence of specific cell types in particular locations or gene expression patterns that determine responses to local perturbations or exogenous insults (Rinn et al., 2008). In the mouse, a similar heterogeneity in function is determined by site-specific requirements such as physical stress, barrier function, or immune responses. Previous studies have shown that susceptibility to development of skin tumors is dependent on location. Transgenic approaches in which keratin gene

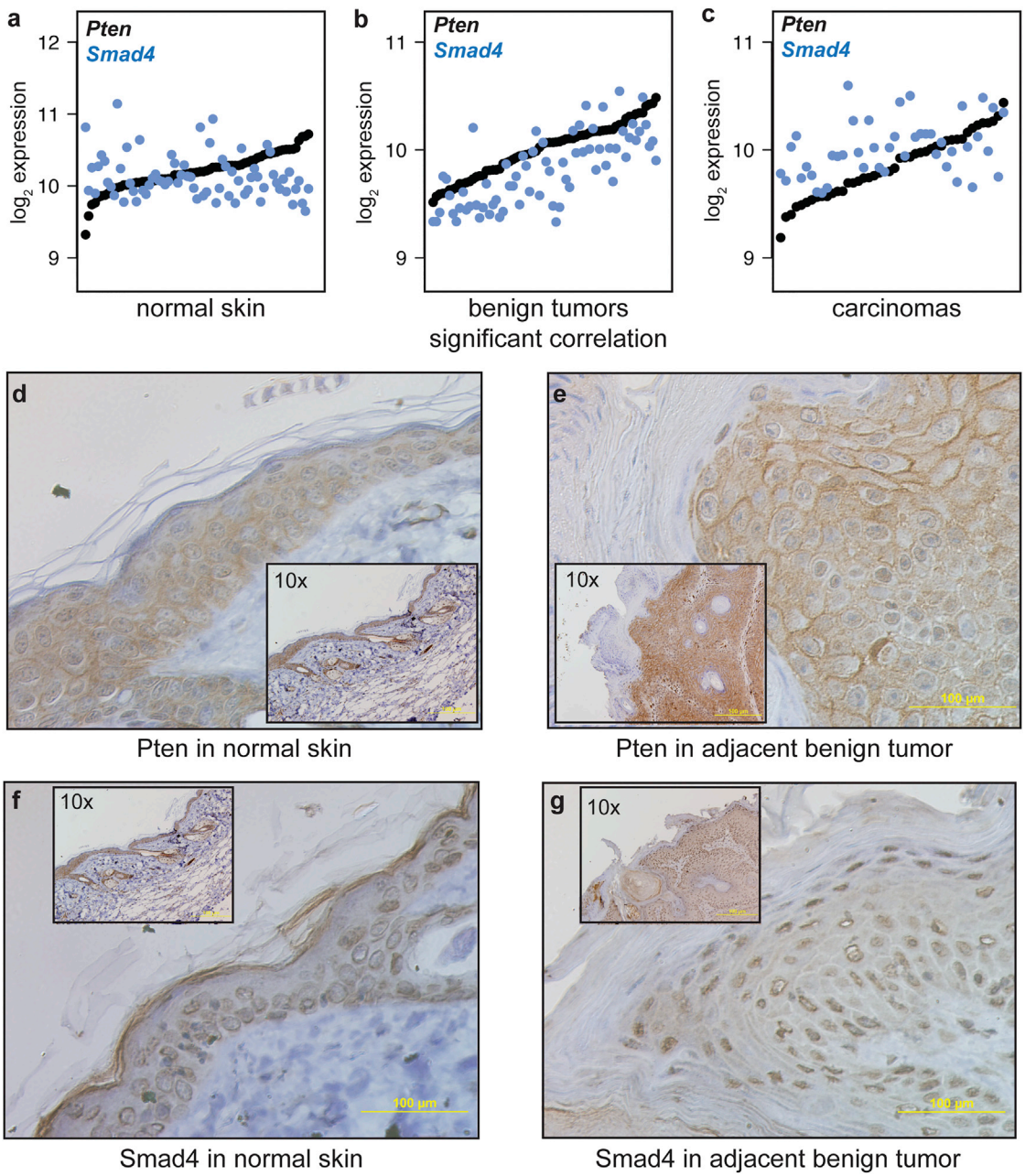

Figure 5. Tumor Suppressor Gene Rewiring during Tumorigenesis

(A–C) Expression of Pten and Smad4 in normal skin, benign tumors, and malignant carcinomas showing significant correlation in benign tumors, but not normal skin or malignant carcinomas.

(D–G) Immunohistochemistry of adjacent normal skin (D and F) and benign tumors (E and G) shown at 40× (insets at 10×).

promoters were used to drive expression of oncogenes in skin demonstrated preferential induction of tumors at specific sites, in spite of widespread expression of the gene promoters used. For example, expression of mutant *Hras* under the control of a keratin 5 promoter led to squamous tumors of the back and sometimes ventral skin (Wakabayashi et al., 2007), whereas activation of mutant Smo in cells expressing keratin 14 gave rise to BCCs mainly in tail or ear skin (Wong and Reiter, 2011; Youssef et al., 2012). Chemical carcinogenesis studies also showed that dorsal skin, but not tail skin, is susceptible to squamous tumor development (Schweizer and Marks, 1977b).

In the present study we have explored the basis for these site-specific functional differences using gene expression network analysis of dorsal and tail skins from a genetically heterogeneous mouse population. Randomized inheritance of polymorphic variants between the strongly divergent *Mus musculus* and *Mus*

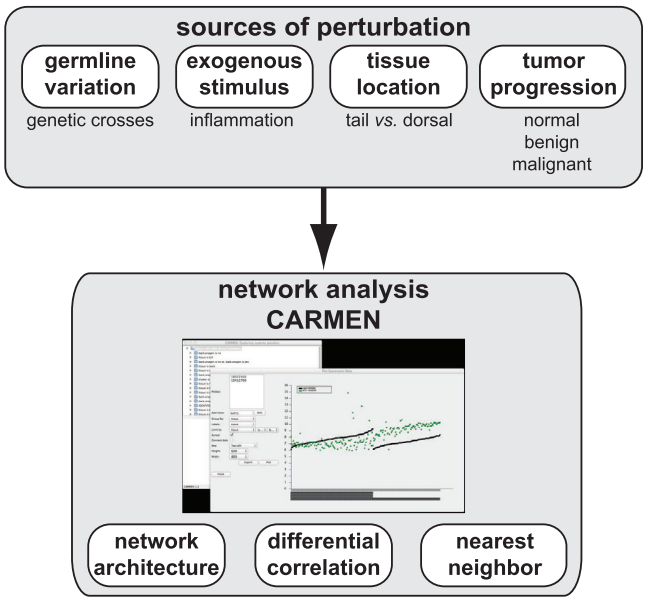

Figure 6. Summary of Network Analysis and Perturbations Presented in This Study

CARMEN can be used to analyze the network architecture of tissue in homeostasis and how that architecture changes in response to stimulation. Gene co-expression networks can be determined from tissue affected by systemic perturbations, including genetic variation, exogenous stimulation, tissue-specific differences, and disease progression.

spretus (Dejager et al., 2009) produced high variance in gene expression between normal individuals. Measuring the co-variation of these genes allowed us to visualize the network architecture of normal skin in two physically and functionally distinct locations.

Analysis of genetic control of gene expression in age- and gender-matched mice showed that the statistical strength of eQTL calculated in 89 tail skins was much higher than that of eQTL calculated from the same number of dorsal skins. Surprisingly, the stronger eQTL were not enriched for roles in either hair follicle control or in cell populations such as Langerhans cells that differ in frequency between tail and dorsal. We found genes with stronger eQTL in tail had roles in ribosomal structure, translation, and energy metabolism. We hypothesize that the apparently constitutive anagen at 8 weeks of age in tail skin plays an important part in explaining this result and is a key difference between tail and dorsal skin overall. While most dorsal tissue samples at this time point were in telogen, each tail sample contained at least some anagen activity. The constitutive anagen and increased proliferative activity of tail skin may allow for clearer dissection of genetic differences between the parental strains.

Differential Cancer Susceptibility in Dorsal and Tail Skin

There is considerable debate over the cellular origins of skin BCCs, with some studies favoring the interfollicular epidermis (Wong and Reiter, 2011; Youssef et al., 2010), the hair follicle bulge region (Wang et al., 2011), or both locations (Grachtchouk et al., 2011). Direct comparison of these results is complicated by the differences in the mouse models used to induce BCCs by targeting oncogene expression or tumor suppressor loss to specific subpopulations of cells in the skin. We set out to address a slightly different question, which is why expression of activated Smo using a Krt14 promoter that is universally active in interfollicular basal cells of both dorsal and tail skin gives rise to BCCs mainly in the tail skin (Wong and Reiter, 2011; Youssef et al., 2010). Our expression analysis identified a network of genes linked to *Smo* expression in tail, but not dorsal, skin that included components of the *Wnt/Lef1* and *Shh* signaling pathways. While many questions remain to be addressed regarding the cellular origins of skin BCCs and SCCs, we propose that mutant Smo activated by *K14*-Cre may have a stronger effect in tail keratinocytes because of the specific wiring of the Smo gene expression pattern in this tissue. Analyses of other Shh signaling components may reveal tissue- or cell-type-specific patterns that could explain the diverse phenotypes observed when carcinomas are induced by different driver genes in subpopulations of skin target cells (Peterson et al., 2015). Loss of *Ptch1* can also lead to BCC formation, but primarily in dorsal rather than tail skin (Wang et al., 2011). The explanation of this phenotype is unknown, but it could be due to differential wiring of the *Ptch1* gene network in dorsal and tail skin or to differences in levels of expression of alternative genes, such as *Ptch2,* that can compensate for loss of *Ptch1* (Adolphe et al., 2014). Indeed, while *Ptch1* mRNA levels are similar in dorsal and tail skins, *Ptch2* is expressed at a significantly higher level in the tails (data not shown), suggesting that compensation may explain the relative lack of tail BCCs when *Ptch1* is deleted in this tissue.

Network Changes during Development of Premalignancy

Mouse models of skin cancer initiated by the carcinogen DMBA display a high specificity for activation of the *Hras* gene by mutation at codon 61 (Bizub et al., 1986; Quintanilla et al., 1986). This event can be circumvented in mice lacking expression of the Pten tumor suppressor gene in keratinocytes (Mao et al., 2004), suggesting a connection between the *Hras* and *Pten* signaling pathways. It was therefore of interest that an unbiased screen for differentially correlated genes in normal skin and *Hras* mutant papillomas from the same backcross mouse population (Quigley et al., 2011) identified *Pten* as one of the top rewired genes, in spite of minimal changes in mRNA expression levels during tumor development. In premalignant papillomas, *Pten* is correlated with a set of genes implicated in alternative tumor suppressor pathways, including the *Trp53* (*Rps26*) and *Tgfß* (*Smad4*) pathways. However, these correlations are disrupted in malignant carcinomas, suggesting that this concerted suppressor network response to *Hras* mutation has to be removed to permit tumor progression. The mechanisms involved are not presently clear, but they do not appear to include direct mutations in *Pten* as shown by exome analysis of benign and malignant skin tumors (McCreery et al., 2015).

These observations demonstrate how network analysis of gene expression can reveal pathway engagement not obvious from differential expression analysis (Figure 6). Methods such as correlation analysis that identify relationships between

genes in the same compartment or across compartments in intact tissues are a useful tool to understand the interactions that underlie normal tissue homeostasis, responses to damage, and development of progressive diseases, including neoplasia.

EXPERIMENTAL PROCEDURES

Animal Breeding and Tissue Collection

FVBBX mice were generated by breeding ([FVB/N × SPRET/Ei] × FVB/N). Mice were housed in standard conditions, fed ad libitum, and sacrificed at 8 weeks of age. Animals were housed and treated in accordance with the regulations and protocols stipulated by the University of California, San Francisco (UCSF) Institutional Animal Care and Use Committee (IACUC). For TPA treatment, the dorsal skins of FVB/N, Spret/Ei, and FVB/N × Spret/Ei mice were shaved and treated 2 days later with a single dose of TPA (200 ml of 10^{-4} M solution in acetone) or vehicle alone. Mice were sacrificed at 0, 2, 4, 6, 24, 48, and 72 hr and after 1 week. Tissue was flash-frozen in liquid nitrogen and stored at −80°C.

Microarray Analysis

RNA was isolated using TRIzol (Invitrogen) according to the manufacturer's instructions. Residual genomic DNA was removed by DNase treatment (Ambion). RNA quality was assessed using a Bioanalyzer (Agilent). Gene expression was quantified using Affymetrix MoGene ST 1.1 arrays hybridized on an Affymetrix GeneTitan instrument. Batch effects were reduced using ComBat (Johnson et al., 2007). Affymetrix MoGene arrays were normalized using the *oligo* package (Carvalho and Irizarry, 2010) and a probe database prepared for FVBBX mice to avoid probes that intersect known FVB/N or Spret/Ei SNPs (Quigley, 2015). Probesets expressed below background levels (determined by expression of Y chromosome genes in female animals) or that did not map to RefSeq-annotated locations for genes were discarded. Multiple probesets assigned to the same gene were collapsed to one signal using the following rule: If two or more probesets had correlation >0.8, these were combined by their mean and other probesets discarded. If no two probesets had correlation >0.8, the probeset with the highest variance was used and other probesets discarded. Normal/papilloma/carcinoma data were downloaded from GEO (GEO: GSE21264). Raw FVBBX microarray data are available for download at GEO as well (GEO: GSE52650).

Statistical Methods

Spearman rank correlation 5% genome-wide significance was established by permutation (Churchill and Doerge, 1994). Statistical calculations were performed in the R statistical environment (R Core Team, 2012) and CARMEN. Differential expression was tested with SAM (Tusher et al., 2001). Differential correlation was calculated in CARMEN using Fisher's transformation of Spearman rank correlation to determine the significance of a change in correlation between two conditions. Multiple test correction was performed by applying a Bonferroni correction to the number of gene pairs considered. Correlation networks were displayed with Cytoscape 3.2 (Shannon et al., 2003). Genotypes were measured with 240 custom-designed Applied Biosystems TaqMan probes that distinguish the FVB/N and Spret/Ei genomes, measured using the Wafergen platform (http://www.wafergen.com). Genotypes were called using the manufacturer's software. Erroneously called genotypes were corrected and missing genotype data imputed using R/QTL package (Broman et al., 2003). eQTL analysis was performed using CARMEN as described previously (Quigley et al., 2009). CARMEN software and documentation are available at http://davidquigley.com/carmen with source code available at https://github.com/DavidQuigley/QuantitativeGenetics. CARMEN is written in C++ using the wxWidgets and Boost libraries (http://wxwidgets.org; http://www.boost.org). For each gene, association with genotype was tested within a chromosome by linear regression, with gene-wise significance assessed by permutation testing and genome-wide significance tested using permutation p values as input to the *qvalue* package (Storey and Tibshirani, 2003). eQTL LOD plots were generated with R/QTL (Broman et al., 2003). Differential correlation significance was assessed by Bonferroni correction of the Spearman correlation p value for the number of gene pairs considered.

Tissue Staining

For Lrig1 and Krt79 staining, 5-μm skin sections were deparaffinized, and antigen retrieval was performed in 10 mM sodium citrate solution (pH 6) or in Trilogy pre-treatment solution (Cell Marque). Sections were blocked for 1 hr at room temperature with 10% donkey serum (Abcam) diluted in PBS containing 0.3% Triton X-100 and incubated overnight with primary antibodies against Lrig1 (goat, R&D) or Krt79 (rabbit, Abcam) at 4°C. After washing in PBS, sections were incubated with blocking solution containing an Alexa Flour 555-conjugated donkey anti-goat/rabbit secondary antibody (Molecular Probes) and DAPI for 1 hr at room temperature. After another PBS wash, slides were mounted using Citifluor. For other staining, tissues were fixed overnight in 4% paraformaldehyde (PFA) and embedded in paraffin. H&E stains were prepared by the UCSF Gladstone core facility with a Leica ST 5020 multistainer. For immunofluorescence, slides were depariffinized with citrisolve. Antigen retrieval was performed with citrate. Slides were blocked in 10% goat serum (50062Z, Invitrogen) with 0.3% Triton. The primary antibody was rabbit anti-Smo (1:200, Abcam) overnight, followed by secondary antibody conjugated with Alexa Fluor 555 (1:500, Invitrogen) and DAPI (Vectashield, Vector Laboratories).

ACCESSION NUMBERS

The accession number for the raw FVBBX microarray data reported in this paper is GEO: GSE52650.

SUPPLEMENTAL INFORMATION

Supplemental Information includes Supplemental Experimental Procedures, one figure, and six tables and can be found with this article online at http://dx.doi.org/10.1016/j.celrep.2016.06.061.

AUTHOR CONTRIBUTIONS

A.B. designed and oversaw the experiments. D.A.Q. performed the genetic and genomic analyses and wrote CARMEN. R.D. performed animal husbandry. G.L.H., K.D.H., and D.W. contributed to genotyping and DNA/RNA extraction. F.P., J.S., and R.D. performed the TPA time course experiment. C.E.W., P.H., and E.K. performed immunofluorescence. A.K. contributed basal cell carcinoma model data. D.A.Q. and A.B. wrote the manuscript.

ACKNOWLEDGMENTS

A.B. acknowledges support from NCI grants CA84244, CA141455, CA184510, and CA176287 and Darrin Stuart and Nancy Pryer of the Novartis Institutes for Biomedical Research. We thank Ervin Epstein for sharing BCC tissue samples and Peter Vuong and Douglas Chin for technical assistance.

Received: January 7, 2015
Revised: March 16, 2016
Accepted: June 14, 2016
Published: July 14, 2016

REFERENCES

Adolphe, C., Nieuwenhuis, E., Villani, R., Li, Z.J., Kaur, P., Hui, C.C., and Wainwright, B.J. (2014). Patched 1 and patched 2 redundancy has a key role in regulating epidermal differentiation. J. Invest. Dermatol. *134*, 1981–1990.

Arwert, E.N., Hoste, E., and Watt, F.M. (2012). Epithelial stem cells, wound healing and cancer. Nat. Rev. Cancer *12*, 170–180.

Balmain, A., Alonso, A., and Fischer, J. (1977). Histone phosphorylation and synthesis of DNA and RNA during phases of proliferation and differentiation induced in mouse epidermis by the tumor promoter 12-O-tetradecanoyl-phorbol-13-acetate. Cancer Res. *37*, 1548–1555.

Bergstresser, P.R., Fletcher, C.R., and Streilein, J.W. (1980). Surface densities of Langerhans cells in relation to rodent epidermal sites with special immunologic properties. J. Invest. Dermatol. *74*, 77–80.

Bizub, D., Wood, A.W., and Skalka, A.M. (1986). Mutagenesis of the Ha-ras oncogene in mouse skin tumors induced by polycyclic aromatic hydrocarbons. Proc. Natl. Acad. Sci. USA *83*, 6048–6052.

Blanpain, C., and Fuchs, E. (2006). Epidermal stem cells of the skin. Annu. Rev. Cell Dev. Biol. *22*, 339–373.

Bowden, P.E., Haley, J.L., Kansky, A., Rothnagel, J.A., Jones, D.O., and Turner, R.J. (1995). Mutation of a type II keratin gene (K6a) in pachyonychia congenita. Nat. Genet. *10*, 363–365.

Braun, R., Cope, L., and Parmigiani, G. (2008). Identifying differential correlation in gene/pathway combinations. BMC Bioinformatics *9*, 488.

Broman, K.W., Wu, H., Sen, S., and Churchill, G.A. (2003). R/qtl: QTL mapping in experimental crosses. Bioinformatics *19*, 889–890.

Carvalho, B.S., and Irizarry, R.A. (2010). A framework for oligonucleotide microarray preprocessing. Bioinformatics *26*, 2363–2367.

Cheng, J., Syder, A.J., Yu, Q.C., Letai, A., Paller, A.S., and Fuchs, E. (1992). The genetic basis of epidermolytic hyperkeratosis: a disorder of differentiation-specific epidermal keratin genes. Cell *70*, 811–819.

Chiang, C., Swan, R.Z., Grachtchouk, M., Bolinger, M., Litingtung, Y., Robertson, E.K., Cooper, M.K., Gaffield, W., Westphal, H., Beachy, P.A., and Dlugosz, A.A. (1999). Essential role for Sonic hedgehog during hair follicle morphogenesis. Dev. Biol. *205*, 1–9.

Choi, Y., and Kendziorski, C. (2009). Statistical methods for gene set co-expression analysis. Bioinformatics *25*, 2780–2786.

Chu, S., DeRisi, J., Eisen, M., Mulholland, J., Botstein, D., Brown, P.O., and Herskowitz, I. (1998). The transcriptional program of sporulation in budding yeast. Science *282*, 699–705.

Churchill, G.A., and Doerge, R.W. (1994). Empirical threshold values for quantitative trait mapping. Genetics *138*, 963–971.

Cui, D., Li, L., Lou, H., Sun, H., Ngai, S.M., Shao, G., and Tang, J. (2014). The ribosomal protein S26 regulates p53 activity in response to DNA damage. Oncogene *33*, 2225–2235.

DasGupta, R., and Fuchs, E. (1999). Multiple roles for activated LEF/TCF transcription complexes during hair follicle development and differentiation. Development *126*, 4557–4568.

de la Fuente, A. (2010). From 'differential expression' to 'differential networking' - identification of dysfunctional regulatory networks in diseases. Trends Genet. *26*, 326–333.

Dejager, L., Libert, C., and Montagutelli, X. (2009). Thirty years of Mus spretus: a promising future. Trends Genet. *25*, 234–241.

Diepgen, T.L., and Mahler, V. (2002). The epidemiology of skin cancer. Br. J. Dermatol. *146* (*Suppl 61*), 1–6.

Ding, Z., Wu, C.-J., Chu, G.C., Xiao, Y., Ho, D., Zhang, J., Perry, S.R., Labrot, E.S., Wu, X., Lis, R., et al. (2011). SMAD4-dependent barrier constrains prostate cancer growth and metastatic progression. Nature *470*, 269–273.

Doherty, L., Sheen, M.R., Vlachos, A., Choesmel, V., O'Donohue, M.F., Clinton, C., Schneider, H.E., Sieff, C.A., Newburger, P.E., Ball, S.E., et al. (2010). Ribosomal protein genes RPS10 and RPS26 are commonly mutated in Diamond-Blackfan anemia. Am. J. Hum. Genet. *86*, 222–228.

Fischer, H., Langbein, L., Reichelt, J., Praetzel-Wunder, S., Buchberger, M., Ghannadan, M., Tschachler, E., and Eckhart, L. (2014). Loss of keratin K2 expression causes aberrant aggregation of K10, hyperkeratosis, and inflammation. J Invest Dermatol. *134*, 2579–2588.

Fitch, K.R., McGowan, K.A., van Raamsdonk, C.D., Fuchs, H., Lee, D., Puech, A., Hérault, Y., Threadgill, D.W., Hrabé de Angelis, M., and Barsh, G.S. (2003). Genetics of dark skin in mice. Genes Dev. *17*, 214–228.

Fuchs, E. (1995). Keratins and the skin. Annu. Rev. Cell Dev. Biol. *11*, 123–153.

Fürstenberger, G., and Marks, F. (1983). Growth stimulation and tumor promotion in skin. J. Invest. Dermatol. *81* (*1, Suppl*), 157s–162s.

Gat, U., DasGupta, R., Degenstein, L., and Fuchs, E. (1998). De Novo hair follicle morphogenesis and hair tumors in mice expressing a truncated beta-catenin in skin. Cell *95*, 605–614.

Glinka, A., Dolde, C., Kirsch, N., Huang, Y.L., Kazanskaya, O., Ingelfinger, D., Boutros, M., Cruciat, C.M., and Niehrs, C. (2011). LGR4 and LGR5 are R-spondin receptors mediating Wnt/β-catenin and Wnt/PCP signalling. EMBO Rep. *12*, 1055–1061.

Grachtchouk, M., Mo, R., Yu, S., Zhang, X., Sasaki, H., Hui, C.C., and Dlugosz, A.A. (2000). Basal cell carcinomas in mice overexpressing Gli2 in skin. Nat. Genet. *24*, 216–217.

Grachtchouk, M., Pero, J., Yang, S.H., Ermilov, A.N., Michael, L.E., Wang, A., Wilbert, D., Patel, R.M., Ferris, J., Diener, J., et al. (2011). Basal cell carcinomas in mice arise from hair follicle stem cells and multiple epithelial progenitor populations. J. Clin. Invest. *121*, 1768–1781.

Gu, L.H., and Coulombe, P.A. (2007). Keratin function in skin epithelia: a broadening palette with surprising shades. Curr. Opin. Cell Biol. *19*, 13–23.

Huelsken, J., Vogel, R., Erdmann, B., Cotsarelis, G., and Birchmeier, W. (2001). beta-Catenin controls hair follicle morphogenesis and stem cell differentiation in the skin. Cell *105*, 533–545.

Johnson, W.E., Li, C., and Rabinovic, A. (2007). Adjusting batch effects in microarray expression data using empirical Bayes methods. Biostatistics *8*, 118–127.

Kasper, M., Jaks, V., Are, A., Bergström, Å., Schwäger, A., Svärd, J., Teglund, S., Barker, N., and Toftgård, R. (2011). Wounding enhances epidermal tumorigenesis by recruiting hair follicle keratinocytes. Proc. Natl. Acad. Sci. USA *108*, 4099–4104.

Kishimoto, J., Burgeson, R.E., and Morgan, B.A. (2000). Wnt signaling maintains the hair-inducing activity of the dermal papilla. Genes Dev. *14*, 1181–1185.

Lane, E.B., and McLean, W.H. (2004). Keratins and skin disorders. J. Pathol. *204*, 355–366.

Lessard, J.C., Piña-Paz, S., Rotty, J.D., Hickerson, R.P., Kaspar, R.L., Balmain, A., and Coulombe, P.A. (2013). Keratin 16 regulates innate immunity in response to epidermal barrier breach. Proc. Natl. Acad. Sci. USA *110*, 19537–19542.

Mahmoudi, T., Li, V.S., Ng, S.S., Taouatas, N., Vries, R.G., Mohammed, S., Heck, A.J., and Clevers, H. (2009). The kinase TNIK is an essential activator of Wnt target genes. EMBO J. *28*, 3329–3340.

Mancuso, M., Leonardi, S., Tanori, M., Pasquali, E., Pierdomenico, M., Rebessi, S., Di Majo, V., Covelli, V., Pazzaglia, S., and Saran, A. (2006). Hair cycle-dependent basal cell carcinoma tumorigenesis in Ptc1neo67/+ mice exposed to radiation. Cancer Res. *66*, 6606–6614.

Mao, J.-H., To, M.D., Perez-Losada, J., Wu, D., Del Rosario, R., and Balmain, A. (2004). Mutually exclusive mutations of the Pten and ras pathways in skin tumor progression. Genes Dev. *18*, 1800–1805.

McCreery, M.Q., Halliwill, K.D., Chin, D., Delrosario, R., Hirst, G., Vuong, P., Jen, K.Y., Hewinson, J., Adams, D.J., and Balmain, A. (2015). Evolution of metastasis revealed by mutational landscapes of chemically induced skin cancers. Nat. Med. *21*, 1514–1520.

McLean, W.H., Rugg, E.L., Lunny, D.P., Morley, S.M., Lane, E.B., Swensson, O., Dopping-Hepenstal, P.J., Griffiths, W.A., Eady, R.A., Higgins, C., et al. (1995). Keratin 16 and keratin 17 mutations cause pachyonychia congenita. Nat. Genet. *9*, 273–278.

Miller, S.J., Wei, Z.G., Wilson, C., Dzubow, L., Sun, T.T., and Lavker, R.M. (1993). Mouse skin is particularly susceptible to tumor initiation during early anagen of the hair cycle: possible involvement of hair follicle stem cells. J. Invest. Dermatol. *101*, 591–594.

Müller-Röver, S., Handjiski, B., van der Veen, C., Eichmüller, S., Foitzik, K., McKay, I.A., Stenn, K.S., and Paus, R. (2001). A comprehensive guide for the accurate classification of murine hair follicles in distinct hair cycle stages. J. Invest. Dermatol. *117*, 3–15.

Nabors, G.S., and Farrell, J.P. (1994). Site-specific immunity to Leishmania major in SWR mice: the site of infection influences susceptibility and expression of the antileishmanial immune response. Infect. Immun. *62*, 3655–3662.

Page, M.E., Lombard, P., Ng, F., Göttgens, B., and Jensen, K.B. (2013). The epidermis comprises autonomous compartments maintained by distinct stem cell populations. Cell Stem Cell *13*, 471–482.

Paramio, J.M., and Jorcano, J.L. (2002). Beyond structure: do intermediate filaments modulate cell signalling? BioEssays *24*, 836–844.

Paus, R., van der Veen, C., Eichmüller, S., Kopp, T., Hagen, E., Müller-Röver, S., and Hofmann, U. (1998). Generation and cyclic remodeling of the hair follicle immune system in mice. J. Invest. Dermatol. *111*, 7–18.

Peterson, S.C., Eberl, M., Vagnozzi, A.N., Belkadi, A., Veniaminova, N.A., Verhaegen, M.E., Bichakjian, C.K., Ward, N.L., Dlugosz, A.A., and Wong, S.Y. (2015). Basal cell carcinoma preferentially arises from stem cells within hair follicle and mechanosensory niches. Cell Stem Cell *16*, 400–412.

Quigley, D. (2015). Equalizer reduces SNP bias in Affymetrix microarrays. BMC Bioinformatics *16*, 238.

Quigley, D.A., To, M.D., Pérez-Losada, J., Pelorosso, F.G., Mao, J.H., Nagase, H., Ginzinger, D.G., and Balmain, A. (2009). Genetic architecture of mouse skin inflammation and tumour susceptibility. Nature *458*, 505–508.

Quigley, D.A., To, M.D., Kim, I.J., Lin, K.K., Albertson, D.G., Sjolund, J., Pérez-Losada, J., and Balmain, A. (2011). Network analysis of skin tumor progression identifies a rewired genetic architecture affecting inflammation and tumor susceptibility. Genome Biol. *12*, R5.

Quintanilla, M., Brown, K., Ramsden, M., and Balmain, A. (1986). Carcinogen-specific mutation and amplification of Ha-ras during mouse skin carcinogenesis. Nature *322*, 78–80.

R Core Team (2012). R: A Language and Environment for Statistical Computing (R Foundation for Statistical Computing).

Reiners, J.J., Jr., and Slaga, T.J. (1983). Effects of tumor promoters on the rate and commitment to terminal differentiation of subpopulations of murine keratinocytes. Cell *32*, 247–255.

Rentrop, M., Nischt, R., Knapp, B., Schweizer, J., and Winter, H. (1987). An unusual type-II 70-kilodalton keratin protein of mouse epidermis exhibiting postnatal body-site specificity and sensitivity to hyperproliferation. Differentiation *34*, 189–200.

Rinn, J.L., Wang, J.K., Liu, H., Montgomery, K., van de Rijn, M., and Chang, H.Y. (2008). A systems biology approach to anatomic diversity of skin. J. Invest. Dermatol. *128*, 776–782.

Rothnagel, J.A., Dominey, A.M., Dempsey, L.D., Longley, M.A., Greenhalgh, D.A., Gagne, T.A., Huber, M., Frenk, E., Hohl, D., and Roop, D.R. (1992). Mutations in the rod domains of keratins 1 and 10 in epidermolytic hyperkeratosis. Science *257*, 1128–1130.

Salmena, L., Carracedo, A., and Pandolfi, P.P. (2008). Tenets of PTEN tumor suppression. Cell *133*, 403–414.

Schlingemann, J., Hess, J., Wrobel, G., Breitenbach, U., Gebhardt, C., Steinlein, P., Kramer, H., Fürstenberger, G., Hahn, M., Angel, P., and Lichter, P. (2003). Profile of gene expression induced by the tumour promotor TPA in murine epithelial cells. Int. J. Cancer *104*, 699–708.

Schneider, M.R., Schmidt-Ullrich, R., and Paus, R. (2009). The hair follicle as a dynamic miniorgan. Curr. Biol. *19*, R132–R142.

Schweizer, J., and Marks, F. (1977a). A developmental study of the distribution and frequency of Langerhans cells in relation to formation of patterning in mouse tail epidermis. J. Invest. Dermatol. *69*, 198–204.

Schweizer, J., and Marks, F. (1977b). Induction of the formation of new hair follicles in mouse tail epidermis by the tumor promoter 12-O-tetradecanoylphorbol-13-acetate. Cancer Res. *37*, 4195–4201.

Shannon, P., Markiel, A., Ozier, O., Baliga, N.S., Wang, J.T., Ramage, D., Amin, N., Schwikowski, B., and Ideker, T. (2003). Cytoscape: a software environment for integrated models of biomolecular interaction networks. Genome Res. *13*, 2498–2504.

Shitashige, M., Satow, R., Jigami, T., Aoki, K., Honda, K., Shibata, T., Ono, M., Hirohashi, S., and Yamada, T. (2010). Traf2- and Nck-interacting kinase is essential for Wnt signaling and colorectal cancer growth. Cancer Res. *70*, 5024–5033.

St-Jacques, B., Dassule, H.R., Karavanova, I., Botchkarev, V.A., Li, J., Danielian, P.S., McMahon, J.A., Lewis, P.M., Paus, R., and McMahon, A.P. (1998). Sonic hedgehog signaling is essential for hair development. Curr. Biol. *8*, 1058–1068.

Steinert, P.M., Steven, A.C., and Roop, D.R. (1985). The molecular biology of intermediate filaments. Cell *42*, 411–420.

Stenn, K.S., and Paus, R. (2001). Controls of hair follicle cycling. Physiol. Rev. *81*, 449–494.

Storey, J.D., and Tibshirani, R. (2003). Statistical significance for genomewide studies. Proc. Natl. Acad. Sci. USA *100*, 9440–9445.

Suzuki, A., Itami, S., Ohishi, M., Hamada, K., Inoue, T., Komazawa, N., Senoo, H., Sasaki, T., Takeda, J., Manabe, M., et al. (2003). Keratinocyte-specific Pten deficiency results in epidermal hyperplasia, accelerated hair follicle morphogenesis and tumor formation. Cancer Res. *63*, 674–681.

Tong, P.L., Roediger, B., Kolesnikoff, N., Biro, M., Tay, S.S., Jain, R., Shaw, L.E., Grimbaldeston, M.A., and Weninger, W. (2014). The skin immune atlas: three-dimensional analysis of cutaneous leukocyte subsets by multiphoton microscopy. J. Invest. Dermatol. *135*, 84–93.

Tusher, V.G., Tibshirani, R., and Chu, G. (2001). Significance analysis of microarrays applied to the ionizing radiation response. Proc. Natl. Acad. Sci. USA *98*, 5116–5121.

Veniaminova, N.A., Vagnozzi, A.N., Kopinke, D., Do, T.T., Murtaugh, L.C., Maillard, I., Dlugosz, A.A., Reiter, J.F., and Wong, S.Y. (2013). Keratin 79 identifies a novel population of migratory epithelial cells that initiates hair canal morphogenesis and regeneration. Development *140*, 4870–4880.

Wakabayashi, Y., Mao, J.-H., Brown, K., Girardi, M., and Balmain, A. (2007). Promotion of Hras-induced squamous carcinomas by a polymorphic variant of the Patched gene in FVB mice. Nature *445*, 761–765.

Wang, G.Y., Wang, J., Mancianti, M.L., and Epstein, E.H., Jr. (2011). Basal cell carcinomas arise from hair follicle stem cells in Ptch1(+/-) mice. Cancer Cell *19*, 114–124.

Wang, Y., Szretter, K.J., Vermi, W., Gilfillan, S., Rossini, C., Cella, M., Barrow, A.D., Diamond, M.S., and Colonna, M. (2012). IL-34 is a tissue-restricted ligand of CSF1R required for the development of Langerhans cells and microglia. Nat. Immunol. *13*, 753–760.

Watson, M. (2006). CoXpress: differential co-expression in gene expression data. BMC Bioinformatics *7*, 509.

Wong, S.Y., and Reiter, J.F. (2011). Wounding mobilizes hair follicle stem cells to form tumors. Proc. Natl. Acad. Sci. USA *108*, 4093–4098.

Xu, X., Ehdaie, B., Ohara, N., Yoshino, T., and Deng, C.-X. (2010). Synergistic action of Smad4 and Pten in suppressing pancreatic ductal adenocarcinoma formation in mice. Oncogene *29*, 674–686.

Yang, L., Mao, C., Teng, Y., Li, W., Zhang, J., Cheng, X., Li, X., Han, X., Xia, Z., Deng, H., and Yang, X. (2005). Targeted disruption of Smad4 in mouse epidermis results in failure of hair follicle cycling and formation of skin tumors. Cancer Res. *65*, 8671–8678.

Youssef, K.K., Van Keymeulen, A., Lapouge, G., Beck, B., Michaux, C., Achouri, Y., Sotiropoulou, P.A., and Blanpain, C. (2010). Identification of the cell lineage at the origin of basal cell carcinoma. Nat. Cell Biol. *12*, 299–305.

Youssef, K.K., Lapouge, G., Bouvrée, K., Rorive, S., Brohée, S., Appelstein, O., Larsimont, J.C., Sukumaran, V., Van de Sande, B., Pucci, D., et al. (2012). Adult interfollicular tumour-initiating cells are reprogrammed into an embryonic hair follicle progenitor-like fate during basal cell carcinoma initiation. Nat. Cell Biol. *14*, 1282–1294.

Zhu, Y., Poyurovsky, M.V., Li, Y., Biderman, L., Stahl, J., Jacq, X., and Prives, C. (2009). Ribosomal protein S7 is both a regulator and a substrate of MDM2. Mol. Cell *35*, 316–326.